Dual B-spline Snake for Interactive Myocardial Segmentation

Kevin Bianchi[1,2]

Antoine Vacavant[1]

Robin Strand[3]

Pierre Terve[2]

Laurent Sarry[1]

[1] ISIT UMR6284 CNRS, Univ. d'Auvergne BP10448, F-63000 Clermont-Ferrand

[2] KEOSYS Company 1, impasse Auguste Fresnel, F 44815 Saint Herblain

[3] Centre for Image Analysis, Uppsala University, Sweden

Abstract

This paper presents a novel interactive segmentation formalism based on two coupled B-Spline snake models to efficiently and simultaneously extract myocardial walls from short-axis magnetic resonance images. The main added value of this model is interaction as it is possible to quickly and intuitively correct the result in complex cases without restarting the whole segmentation working flow. During this process, energies computed from the images guide the user to the best position of the model.

1 Introduction

In order to detect myocardial walls from short-axis MR images, classical methods use image gradient driven forces [3, 15], but these methods are known to be sensitive to noise and to have restricted spatial extension. Thus region-based terms as region homogeneity have been introduced more recently [4, 13] as a remedy. To make gradient-based terms more robust, the Gradient Vector Flow (GVF) [16] obtained by diffusion of the gradient vector field in homogeneous regions is used in [8]. In [9], it is employed for joint propagation of endocardium and epicardium contours in a levelset framework. The Deformable Elastic Template [6] is a finite element model that simulates heart mechanical behaviour in a linear elasticity setting. Image forces are also computed from GVF terms at the boundaries. For most of these methods, user interaction options are often limited to the choice of few points on the first slice or to the manual delineation of the first contour location [14].

The core of the article is organized as follows: In Section 2, we introduce segmentation assumptions related to myocardium detection and tracking, then the principles of our new deformable model (geometrical constraints and energies), called dual B-spline model. Finally, we show the results provided by the dual B-spline model in Section 3, as well as the ability to quickly correct the result in complex cases.

2 Methodology

Our goal is to simultaneously extract myocardial walls with a formalism that allows interaction to correct the result if an error occurs. The endocardium is the inside wall between the myocardium and the cavity, and has a rather homogeneous gray level, except for the pillars. The epicardium is the outer wall of the myocardium. The external regions are totally inhomogeneous in gray levels, and the contrast of the boundary varies in intensity and even in sign. We thus introduce a coupled heterogeneous energy in agreement with these constraints and a shape energy term to prevent unexpected behaviour.

2.1 Geometric Representation

Dual B-spline Snake

Introduced by Brigger and Unser [10], B-spline Snake is a compact representation that addresses several problems arising from Kass *et al.* Snake model [7] and B-Snake model [12]. The contour model is defined from the nodal points of a B-spline curve. This allows to intuitively and directly control the curve. Moreover, it is possible to convert nodal points to control points and *vice versa* by linear filtering. We use a new interactive model called dual B-spline snake designed to model both myocardial walls. Contrary to existing automatic methods requiring any user to guess the correct initialization to make the model converge, our approach provides a convenient interactive way to correct the result. The two coupled B-Spline contours $\mathbf{C}_{endo}$ and $\mathbf{C}_{epi}$ are defined from a centerline curve $\mathbf{C}_{center}$ at one half thickness b as in the model of Parallel Active Contours [5]:

$$\begin{aligned} \mathbf{C}_{endo}(t) &= \mathbf{C}_{center}(t) - b(t)\mathbf{n}, \\ \mathbf{C}_{epi}(t) &= \mathbf{C}_{center}(t) + b(t)\mathbf{n}, \end{aligned} \tag{1}$$

where $\mathbf{n}$ is the normal of the B-Spline curve $\mathbf{C}_{center}$ and t its parameter.

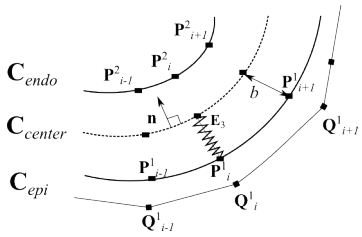

Figure 1: Dual B-spline model: $\mathbf{P}_i^1$, $\mathbf{P}_i^2$ are the nodal points of epicardium and endocardium contours respectively, while $\mathbf{Q}_i^1$ are the control points of epicardium contour.

Sectorization Constraint

Traditionally, the uniformity of B-spline node positions during evolution is ensured by a reparameterization energy [10], avoiding shape singularities. For myocardium segmentation, they could be due to pillars for instance. Given the global convexity of the expected walls, an angular constraint is used: The nodal points are subject to lie on the American Heart Association's (AHA) myocardial sectorization limits usually considered by the cardiologists [1] (Fig. 2). The forces derived from the energy terms are projected onto these directions.

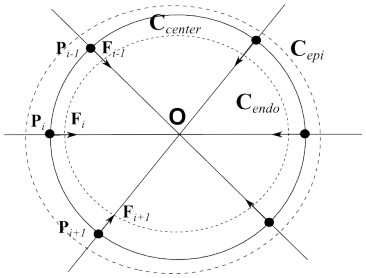

Figure 2: Dual B-spline snake model endocardial contour $\mathbf{C}_{endo}$ and epicardial contour $\mathbf{C}_{epi}$ computed from the centerline contour $\mathbf{C}_{center}$ where forces $\mathbf{F}_i$, deriving from the global energy E (2), are constrained to lie along the AHA sector limits.

2.2 Internal and External Energies

To improve the robustness of endocardium and epicardium segmentations, we have used a new grayscale distance transformation to enhance myocardium and epicardium contrast thanks to the algorithms proposed in [11].
For the evolution of the centerline curve and half width, an energy E made of the combination of three heterogeneous terms is minimized:

$$E = \alpha E_1(\mathbf{C}_{endo}) + \beta E_2(\mathbf{C}_{epi}) + \gamma E_3(\mathbf{C}_{endo}, \mathbf{C}_{epi}), \alpha + \beta + \gamma = 1, \tag{2}$$

where α, β and γ are weighting parameters. $E_1(\mathbf{C}_{endo})$, a region-type energy term of Chan and Vese (CV) [2], is preferred for the endocardium contour, whereas a Gradient Vector Flow (GVF) [16], *i.e.* a boundary-type energy term is chosen for $E_2(\mathbf{C}_{epi})$. As epicardium constraint is sometimes weak in the absence of gradient information, a coupling energy term, $E_3(\mathbf{C}_{endo}, \mathbf{C}_{epi})$, applied between endocardium and epicardium contours, prevents unexpected behaviour and acts as a shape memory term.

Elastic Coupling Energy

An elastic coupling energy, E_3, is used to induce a restoring force, between the two curves (Fig. 1). As exact myocardial thickness is unknown, we make it adaptive by considering an average thickness, *i.e.* energy E_3 is equivalent to the variance of b values. For instance, at nodal point i:

$$E_3(t = t_i) = (b_i - \sum_{j=1}^{M} \frac{b_j}{M})^2, i \in [1, M]. \tag{3}$$

Global Energy Minimization

We describe here how to derivate global energy E with respect to the nodal points of our dual B-spline model. For instance, at nodal point i, we get from (1) and (2):

$$\frac{\partial E}{\partial \mathbf{P}_i(t = t_i)} = \alpha \frac{\partial E_1(\mathbf{C}_{endo})}{\partial \mathbf{P}_i} + \beta \frac{E_2(\mathbf{C}_{epi})}{\partial \mathbf{P}_i}$$

$$= \alpha(\mathbf{Id_2} - b_i \frac{\partial \mathbf{n}^{\mathrm{T}}}{\partial \mathbf{P}_i})\mathbf{F}_{endo}(t_i) + \beta(\mathbf{Id_2} + b_i \frac{\partial \mathbf{n}^{\mathrm{T}}}{\partial \mathbf{P}_i})\mathbf{F}_{epi}(t_i), \tag{4}$$

where $\mathbf{F}_{endo}$ and $\mathbf{F}_{epi}$ are the forces deriving from the energies E_{endo} and E_{epi} respectively. The nodal points of the centerline $\mathbf{C}_{center}$ are subject to a directional constraint along a sector limit $\mathbf{P}_i = \mathbf{O} + \lambda_i \mathbf{c}_i$, where $\mathbf{O}$ is the initial point of the half line, and $\mathbf{c}_i$ is the unit vector of the considered direction. Then the only degree of freedom is λ_i and the corresponding derivative is:

$$\frac{\partial E}{\partial \lambda_i} = \frac{\partial E}{\partial \mathbf{P}_i}\frac{\partial \mathbf{P}_i}{\partial \lambda_i} = \frac{\partial E}{\partial \mathbf{P}_i}\mathbf{c}_i, \tag{5}$$

meaning that the previously computed gradient vector (5) should be projected onto $\mathbf{c}_i$. Then we describe how to derivate the half thickness b_i at nodal point i:

$$\begin{aligned}\frac{\partial E}{\partial b_i(t=t_i)} &= \alpha\frac{\partial E_1(\mathbf{C}_{endo})}{\partial b_i} + \beta\frac{\partial E_2(\mathbf{C}_{epi})}{\partial b_i} + \gamma\frac{\partial E_3(\mathbf{C}_{endo},\mathbf{C}_{epi})}{\partial b_i} \\ &= \alpha\frac{\partial E_1(\mathbf{C}_{endo})}{\partial \mathbf{C}_{endo}}.\mathbf{n} + \beta\frac{\partial E_2(\mathbf{C}_{epi})}{\partial \mathbf{C}_{epi}}.\mathbf{n} + \gamma\frac{\partial E_3(\mathbf{C}_{endo},\mathbf{C}_{epi})}{\partial b_i} \\ &= \left[-\alpha\mathbf{F}_{endo}(t_i) + \beta\mathbf{F}_{epi}(t_i)\right].\mathbf{n} + 2\gamma\frac{M-1}{M}\left(b_i - \sum_{j=1}^{M}\frac{b_j}{M}\right).\end{aligned} \tag{6}$$

For minimization, we have used a gradient descent with constant step. First, the algorithm computes the forces applied to the nodal points of the centerline curve from (4), the new positions of the points, and then the partial derivatives to update the half-thickness using (6). The endocardial and epicardial curves are updated with the new position of the middle curve and the new half-thicknesses using (1).

3 Results and Discussion

To evaluate the segmentation accuracy of the dual B-spline snake, ground truth contours are manually drawn by an expert. We use 4 datasets of 24 slices. Two types of classical indices are computed (Tab. 1): Region superposition indices like Dice Coefficient (DI is a similarity measure between myocardial regions) and Vinet's criterion (VI is a measure of the overlap between myocardial regions); and contour distance metrics like Mean Absolute Distance (MAD gives the global correspondence between contours) and Hausdorff distance (HD gives the maximum symmetric distance between contours).

The values of all the segmentation indices (Tab. 1(a)) are in favour of the accuracy of the proposed method. Errors are mainly due to the GVF field that is distorted by the presence of a strong contrast at pericardium (Fig. 3(b)). On the contrary, the lack of contrast of myocardium (Fig. 3(a)) reduces the segmentation accuracy. Finally, high ejection fraction may significantly reduce the left ventricular area as for the last dataset (Fig. 3(c)). This is the interest of using the interaction capacities of the dual B-spline snake model, in the case of complex situations where automatic segmentation fails.

One only needs to move the nodal points of the curve that are badly positionned, *i.e.* attracted by a local minimum. But this is smart interaction since forces deriving from the image energy terms act like restoring forces against user displacement: They are maximal at the expected contour position, as illustrated in Fig. 4(a). In this case, the user makes our model go over the local minima where it fell (Fig. 4(b)). Table 1(b) shows the errors when user's interactive correction is applied: For datasets 1, 2 and 4 the Haussdorf Distance values are halved. More generally, all the indices are improved.

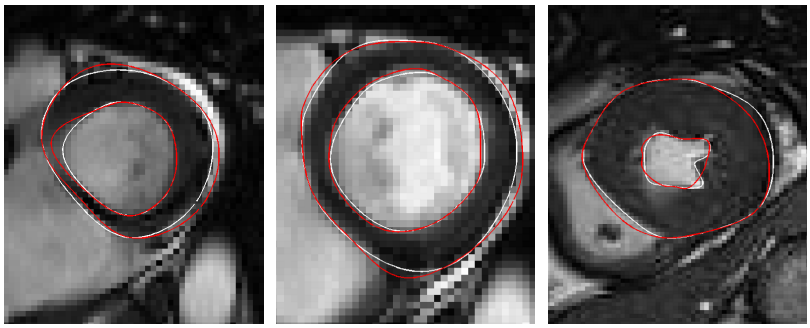

(a) (b) (c)

Figure 3: Myocardial wall segmentation issues with Dual B-Spline Snake (red curves) compared to expert delineation (white curves). a) dataset 1; b) dataset 2; c) dataset 4.

Table 1: Quantitative evaluation vs. ground truth provided by an expert.

(a)

Dataset	DI(%)	VI(%)	HD(pix)	MAD(pix)
1	95.4±0.2	0.14±0.09	1.23±0.90	0.25±0.16
2	97.5±0.2	0.07±0.07	1.29±0.61	0.22±0.16
3	93.5±0.2	0.3 ±0.15	1.84±0.93	0.76±0.30
4	96 ±0.2	0.2 ±0.15	2.74±1.15	0.54±0.35

(b)

Dataset	DI(%)	VI(%)	HD(pix)	MAD(pix)
1	98.9±0.2	0.03±0.02	0.68±0.55	0.03±0.05
2	99.5±0.2	0.02±0.01	0.56±0.52	0.04±0.04
3	94.2±0.2	0.27±0.09	1.67±0.73	0.69±0.21
4	98.6±0.2	0.07±0.13	1.25±1.17	0.19±0.33

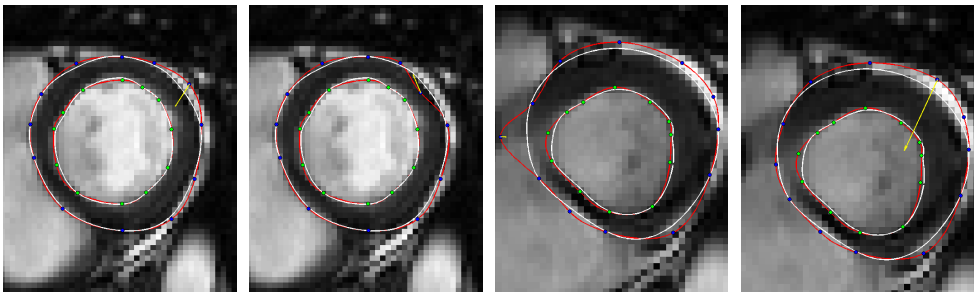

(a) (b) (c) (d)

Figure 4: Displacement of nodal points for interactive contour correction: a,c) the image force direction is the same as user's interaction; b,d) the image force direction is opposite to user's interaction.

The dual B-spline snake we have proposed in this paper is adapted to myocardium seg-

mentation, and allows simple interactive correction. As future works to improve segmentation robustness, methods will be extented to 3D and even to 4D to bring temporal coherence. We also plan to use this model for myocardial tracking by coupling segmentation with motion estimation. For the correction step, the good results show the interest provided by any user's interaction. To increase efficiency of the correction, we would like to use haptic devices to make 3D image restoring forces more perceptible than in a classical slice processing software.

References

[1] M. Cerqueira. Standardized myocardial segmentation and nomenclature for tomographic imaging of the heart: A statement for healthcare professionals from the cardiac imaging committee of the council on clinical cardiology of the american heart association. *J. Nucl. Cardiol.*, 2(9):240–45, 2002.

[2] T. F. Chan and L. Vese. Active contours without edges. *IEEE Trans. on Im. Proc.*, 2(10):266–77, 2001.

[3] A. Gupta et al. Cardiac mr image segmentation using deformable models. *IEEE CCC*, pages 747–50, 1993.

[4] C. Pluempitiwiriyawej et al. Stacs: new active contour scheme for cardiac mr image segmentation. *IEEE Trans. Med. Imag.*, page 24, 2005.

[5] I. Ghorbel et al. Modeling a parallelism constraint in active contours. application to the segmentation of eye vessels and retinal layers. *IEEE ICIP*, pages 445–48, 2011.

[6] J. Schaerer et al. A dynamic elastic model for segmentation and tracking of the heart in mr image sequences. *IEEE WACV*, 14:738–49, 2010.

[7] M. Kass et al. Snakes: Active contour models. *Int. J. Comput. Vis.*, 331:321–31, 1998.

[8] M. Santarelli et al. Automated cardiac mr image segmentation: theory and measurement evaluation. *Med. Eng. Phys.*, page 25, 2003.

[9] N. Paragios et al. Knowledge-based registration and segmentation of the left ventricle: a level set approach. *IEEE WACV*, pages 37–42, 2002.

[10] P. Brigger et al. B-spline snakes: a flexible tool for parametric contour detection. *IEEE Trans. on Im. Proc.*, 9(9):1484–96, 2000.

[11] R. Strand et al. The minimum barrier distance. *Comp. Vis. and Image Underst.*, 2012.

[12] S. Menet et al. B-snakes. implementation and application to stereo. *DARPA*, pages 720–26, 1990.

[13] N. Paragios. A variational approach for the segmentation of the left ventricle in cardiac image analysis. *Int. J. Comput. Vis.*, page 50, 2002.

[14] C. Petitjean and J.N. Dacher. A review of segmentation methods in short axis cardiac mr images, medical image analysis. *IEEE WACV*, 15:169–84, 2011.

[15] S. Ranganath. Contour extraction from cardiac mri studies using snakes. *IEEE Trans. Med. Imag.*, page 14, 1995.

[16] C. Xu and J. L. Prince. Snakes, shapes, and gradient vector flow. *IEEE Trans. on Im. Proc.*, 3(7): 359–69, 1998.